Visual performance using reaction times

Rea, M. S.; Ouellette, M. J.

Publisher's version / Version de l'éditeur:

Lighting Research and Technology, 20, 4, pp. 139-153, 1988

National Research Council Canada
Conseil national de recherches Canada

Institute for Research in Construction
Institut de recherche en construction

NRC·CNRC

Visual Performance Using Reaction Times

by M.S. Rea and M.J. Ouellette

Reprinted from
Lighting Research and Technology
Vol. 20, No. 4, 1988
p. 139-153
(IRC Paper No. 1718)

NRCC 33104

Canada

Lighting Res. Technol. 20(4) 139–153 (1988) Printed in Great Britain

Summary Visual performance has been a topic of study for many years. For a variety of reasons, it has been difficult to develop a completely satisfactory model of visual performance. Recently the connection has been made between reaction time experiments and realistic studies of visual performance. In this report an extensive set of reaction time data are presented which were collected over a large range of stimulus conditions relevant to interior and exterior lighting applications. An empirical model of visual performance was developed from these data. It forms the next logical step in the development of an application tool for lighting practitioners.

Visual performance using reaction times

MARK S REA PhD and MICHAEL J OUELLETTE BSc
National Research Council Canada, Institute for Research in Construction, Ottawa, Ontario, Canada K1A 0R6

Received 1 July 1988, in final form 20 September 1988†

1 Introduction

Although visual performance can have several definitions, it is conventionally defined by the lighting research community as the speed and accuracy of performing a visual task[1]. Speed and accuracy are useful measures of performance and are directly related to productivity. Task performance is more complex than visual performance, however, since it involves motor and cognitive factors as well as visual ones. These factors are also important to productivity. Nevertheless, a person's ability to perform a task requiring sight will be limited if the quality of the visual conditions is poor. The productivity of a typist, for example, will not be satisfactory if the text has insufficient contrast or if its size is small, or if there is inadequate illumination on the document. But what exactly is sufficient text contrast and size? How much illumination is required for satisfactory visual performance?

There have been a number of attempts to answer these important questions over the past half-century. For a variety of reasons outlined by Rea[2,3], earlier attempts have had limited success. For example, Weston's early studies[4,5] using a simulated realistic task followed the correct philosophical path, but the experimental and analytical techniques were poorly defined and, perhaps, poorly executed.[2] Certainly Weston had difficulty in replicating his own results using nominally equivalent procedures. Rea[6] has followed the philosophy of Weston and extended the work on visual performance by incorporating more experimental control and more modern analytical and statistical procedures. The numerical verification task, first used by Smith and Rea[7] and later by others[8–10] has served as a useful simulated realistic task for assessing visual performance. Nevertheless, special experimental and analytical procedures[2,6,8] are required to extract visual performance unambiguously from task performance using the numerical verification task. This is true, of course, for any task, but simulated realistic tasks are particularly difficult in this regard. Reaction times have been used in many areas of perception and psychology to characterise various stages of human information processing[11,12]. Boyce and Rea[13] and Rea *et al*[14] have shown that reaction times can be used to quantify visual performance and, because they have proportionally smaller non-visual contributions to the observed response, there are fewer complications in assessing visual performance using reaction times than with more complex simulated realistic tasks. Further, Rea[8] showed that errors (misses and false-positives) and response times followed very similar, if not identical, functions of target contrast. Similarly, Rea[2] showed that his visual performance model based on speed[6] could predict the visual performance data by McNelis based on accuracy[15]. Therefore, a set of equations for visual performance based upon reaction times is appropriate for predicting visual performance at realistic tasks in terms of both speed and accuracy.

This report extends the previous efforts to model visual performance by presenting data on reaction times for detecting square targets of different contrast, contrast polarity and area over a large range of adaptation luminances. Empirical functions describing the data are presented. These functions can be used to predict visual performance throughout a large range of stimulus conditions typically found in indoor and outdoor environments. Although not discussed here, procedures have been developed for applying these findings to lighting practice[16–18].

2 Methods

2.1 General

Two experiments were conducted, one measuring reaction times to targets darker than the background (decrements) and the other measuring reaction times to targets brighter than the background (increments). In total, 9 subjects, 5 males and 4 females, participated in one or both of the experiments. Every subject was examined for visual defects using a Keystone Ophthalmic Telebinocular and employed in the experiment only if the visual acuity of the left eye was assessed normal or better without optical correction or with a contact lens.

Targets were generated on a video screen (Sony, PVM 1910) 1.68 m from the subject's eye. Figure 1 is a schematic diagram of the apparatus. The screen subtends a visual field 12° wide and 7° high. Every subject viewed the stimulus display with the left eye through a 2 mm diameter artificial pupil, and, depending upon the experimental conditions, a neutral density filter and luminous veil. An opaque patch covered the right eye during the experiment.

On a typical trial a target was displayed on the screen after a brief, random time delay, and the subject pressed a

† The paper is a revised version of one presented to the 1988 National Lighting Conference, Cambridge, UK.

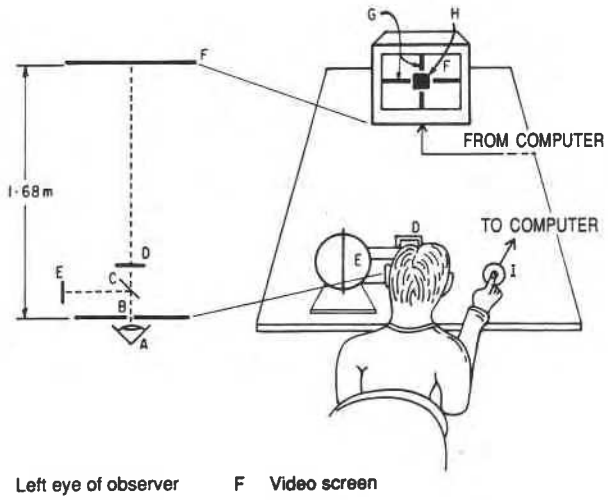

A	Left eye of observer	F	Video screen
B	2 mm artificial pupil	G	Fixation bars
C	Beam splitter	H	Square target
D	Neutral density filter	I	Response button
E	Source of luminous veil		

Figure 1 Schematic diagram of reaction time apparatus

response button as soon as it was detected; a maximum of 3 s was allowed for response. The time between target onset and response was recorded as the reaction time for that trial. Except for setting the adaptation luminances, the two experiments were completely controlled by an IBM PC/XT computer.

Stemming from the conventional definition of contrast $C = |L_b - L_t|/L_b$, where L_t is the target luminance and L_b is the luminance of its background, and taking into account the transmittance (T) of the neutral density filter and the luminance of the veil (L_v):

$$C = \frac{|(TL_b + L_v) - (TL_t + L_v)|}{TL_b + L_v} \quad (1a)$$

or

$$C = \frac{T|L_b - L_t|}{L_a} \quad (1b)$$

where L_a is the adaptation luminance ($cd\,m^{-2}$), equal to $TL_b + L_v$.

To determine L_t and L_b, eight bit pixel intensity values (i.e. 256 steps in luminance) generated by the computer in a 3° field at the centre of the screen were calibrated for luminance using a Minolta Photometer (Model nt−1°). Thus the luminances of targets smaller than the photometer's one-degree measuring field could be determined. The veiling luminance L_v was produced with a beam-splitter just forward of the artificial pupil which reflected light from an integrating sphere (a Photo Research, Spectra luminance standard). Values of L_v, reflected from the beam splitter, were also determined with the Minolta photometer, and a close-up lens, focused at the exit port of the integrating sphere. Filter (Schott optical glass) transmission values (T) were determined, using the Minolta photometer, from luminance measurements of the computer screen, with and without a filter in the optical path.

2.2 *Decrement experiment*

Seven subjects, 3 males and 4 females, between the ages of 17 and 31 years of age (median = 21) participated in the decrement experiment.

The luminance at the centre of the screen was set at 100 $cd\,m^{-2}$. There was a gradual reduction in luminances toward the edge of the screen; luminances in the target presentation area near the centre of the screen varied from 83 to 105 $cd\,m^{-2}$†. Eight luminances were created in combination with the neutral density filters and/or the veiling light (Table 1). Subjects were dark adapted for at least 5 min before starting the experiment.

For every reaction time trial, the computer randomly selected and generated a square target in the centre of four fixation bars (Figure 1). Targets were of eight possible sizes (see Table 7 in Appendix A for target sizes in various units)‡ and of either 18 or 20 possible contrasts. Every subject was presented every target at every adaptation luminance approximately 14 times. Contrast values (equation 1) ranged from near threshold to a possible maximum of 0.99. Although as many as 20 contrasts were employed at each adaptation luminance, the range of apparent contrasts, as seen by the subject, was reduced whenever a veiling light was employed; the greater the veiling luminance (Table 1) the more limited the range of apparent contrasts for the targets.

The onset of the target followed presentation of fixation bars and a subsequent, random time delay between 1 and 3 s. Subjects knew that, on occasion, no target would be presented. This procedure was intended to limit false-positive responses; in fact, the average false-positive rate was 3.5% for these experiments. An inter-trial interval of 1.5 s followed the subject's response to the target. Reaction times were recorded in blocks of 25 trials; a subject initiated each new block at his discretion once the adaptation luminance had been established by the experimenter.

Two horizontal and two vertical fixation bars 0.25° wide extended from the edges of the monitor screen toward the

Table 1 Adaptation luminances L_a and retinal illuminances I_R in the decrement experiment, produced by various combinations of a veiling luminance L_v and a neutral filter placed between the subject and the computer monitor. The maximum contrast values at every adaptation luminance are also tabluated.

L_a ($cd\,m^{-2}$)	$I_R(T)$	Filter transmittance T	L_v ($cd\,m^{-2}$)	Maximum contrast
9.2	29.0	0.0923	0	0.99
16.3	51.2	0.163	0	0.99
24.5	77.0	0.245	0	0.99
46.3	145	0.463	0	0.99
63.1	198	0.463	16.8	0.72
100	314	1	0	0.99
158	496	1	58.5	0.62
255	801	1	155	0.39

† The luminous non-uniformity of the screen was assumed unimportant for defining the adaptation luminance. Of course, the non-uniformity is completely irrelevant for defining target size. It is also irrelevant to defining target contrast, since contrast is dependent upon the ratio of luminances. Any spatially dependent luminance variations in the display cancel in Equation 1.

‡ There was greater measurement uncertainty for the small targets due to phosphor interactions at pixel target borders. More specifically, the targets may have been effectively smaller than the values presented here.

Table 2 Adaptation luminances L_a and retinal illuminances I_R in the increment experiment, produced by various neutral filters placed between the subject and the computer monitor. The maximum contrast was 10.2 for all adaptation luminances.

L_a (cd m^{-2})	I_R(T)	Filter transmittance (T)
0.17	0.534	0.0104
0.77	2.42	0.0475
1.57	4.93	0.0962
8.38	26.3	0.512
16.4	51.5	1

centre forming a 'cross-hair' pattern (Figure 1). Each bar terminated 1.8° from the centre of the monitor screen, defining a blank, square area 3.6° on a side where the stimuli were displayed. The apparent contrast of the fixation bars, as seen by the subject, was constant at 0.6 throughout the experiment, except for the highest adaptation luminance where contrast was only 0.4.

Every subject was presented 19 200 reaction time trials for the decrement experiment. Data collection required approximately 40 h of experimental time and, depending upon the subject, required calendar time of between 2 weeks and 2 months.

2.3 Increment experiment

Seven subjects, 5 male and 2 female, between the ages of 17 and 31 years of age (median = 26) participated in the increment experiment. Five of these subjects also participated in the decrement experiment.

The luminance at the centre of a second computer screen was set at 16.4 cd m^{-2} and fell gradually to 14.1 cd m^{-2} at the edge of the target area. At the extreme edges of the screen, luminances fell to about 10 cd m^{-2}. Five adaptation luminances were employed in the experiment using neutral density filters placed forward of the artificial pupil (Table 2).

At each adaptation luminance, three square targets (0.20, 1.4, and 13 × 10^{-5} steradians) and 16 suprathreshold contrasts (48 possible targets) were presented at random in the centre of four fixation bars; on average, every subject was presented every target at every adaptation luminance approximately 14 times. Contrast values (equation 1) ranged from near threshold to a maximum of 10.2.

The reaction time protocol was identical to that used in the decrement experiment, as were the fixation bars, except the contrast of the fixation bars was 1.5 throughout the experiment.

Every subject was presented 3625 reaction time trials in the experiment. Data collection took approximately 8 h of experimental time, and all data for one subject were usually collected within a week.

§ The contrast ranges for two highest retinal illuminances (Table 1) were limited, so 314 T was chosen to illustrate the differences between a high and a low retinal illuminance.

¶ Each data set was fitted with a single straight line where the 'rise' from a probability of 0.01% to one of 99.9% on the ordinate spanned a $\log_{10}(C)$ 'run' of 1.17 units on the abscissa. The excellent fits by this simple technique obviated more complex numerical methods which would, undoubtedly, have yielded nearly identical estimates of the 50% probability of detection.

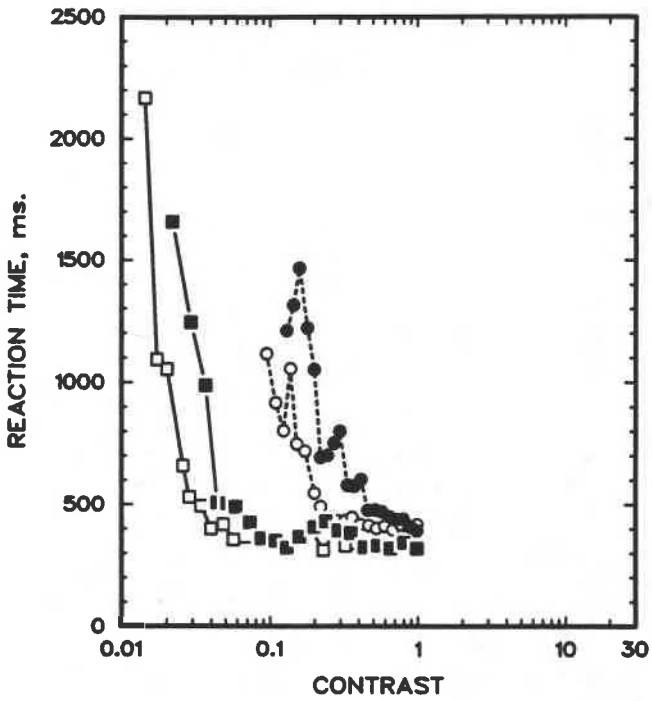

Figure 2 Reaction times from subject 6 to flashed luminous *decrements*. Presented are mean reaction times as a function of target contrast for targets of area 0.20 × 10^{-5} steradians (circles) and 280 × 10^{-5} steradians (squares) at retinal illuminances of 29.0 T (solid symbols) and 314 T (open symbols).

3 Results

3.1 Decrement experiment

Figure 2 shows the results from subject 6; all other subjects gave similar data. Mean reaction times for the largest (280 × 10^{-5} steradians) and smallest (0.20 × 10^{-5} steradians) targets are shown for various contrasts under one of the highest (314 T) and the lowest (29.0 T) retinal illuminances.§

Contrast thresholds were determined by computing the probability of detecting each target. As noted earlier, approximately 14 trials per stimulus condition were presented to every subject. Targets were not always seen by the subjects, and, depending upon the stimulus conditions and the subject, the probability of detecting a given target ranged from near zero to unity. Since the trends in responses from all subjects were similar, the reaction time data from all subjects were combined. The probability of detecting each target of a given size and contrast at all eight retinal illuminances was then computed and the computed probabilities of detection were plotted as a function of $\log_{10}C$. All values (within the range of 1% to 99% probability of detection) for a given combination of target size and retinal illuminance appeared to lie along straight lines of common slope. Figure 3 shows the lines fitted by eye to some of the probability of detection data; all other data were similarly fitted.¶ Using the 50% probability of detection criterion, contrast threshold values were determined using this graphical method for each combination of target size and retinal illuminance. Since the probability-of-detection thresholds are derived from the reaction time experiment they should be more representative of contrast thresholds for the reaction time targets than would those obtained from any other method (e.g. a method of adjustment).

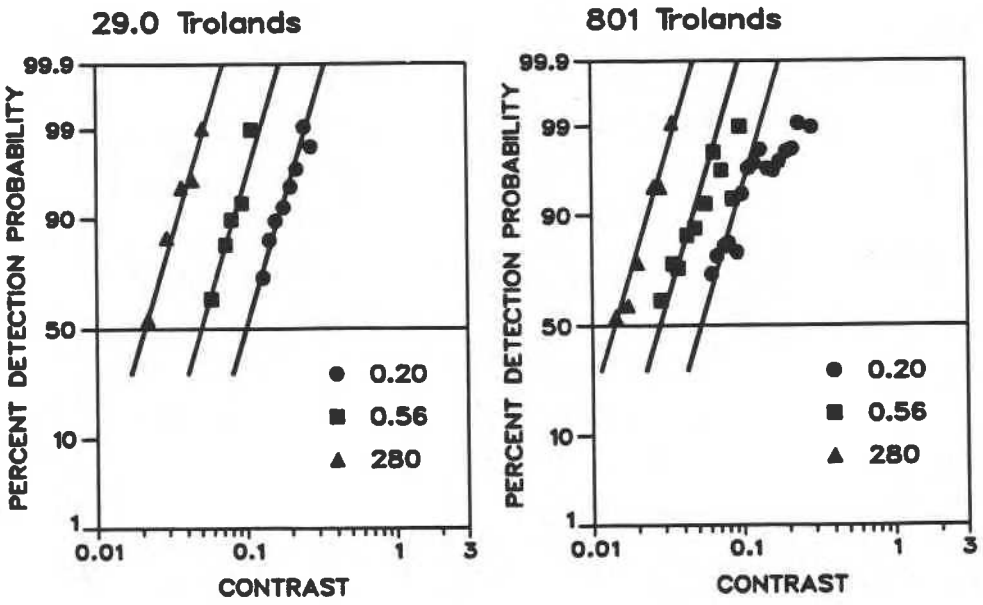

Figure 3 Mean percentage probability-of-detection data for three contrast *decrement* target areas (0.20, 0.56, 280 × 10^{-5} steradians) plotted as a function of $\log_{10}C$ (equation 1) when presented at retinal illuminances of 29.0 and 801 T. A straight line (see text) was fitted by eye to *all* of the probability-of-detection data in the decrement experiment.

Just above threshold contrast, reaction times decrease very rapidly as target contrast increases until a saturation region is reached where still higher target contrasts have little effect. This pattern is particularly evident for large targets and is similar at every level of retinal illuminance used (Figure 2). Reaction times to small targets are typically longer than they are to large targets at the same retinal illuminance. Although less apparent from Figure 2, retinal illuminance more strongly affects the pattern of reaction times for small targets than for large targets.

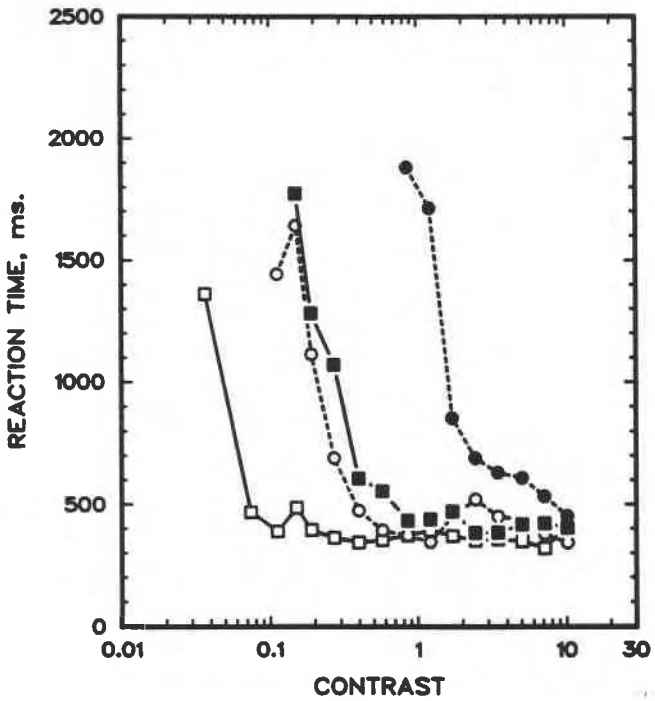

Figure 4 Reaction times from subject 6 to flashed luminous *increments*. Presented are mean reaction times as a function of target contrast for targets of area 13 × 10^{-5} steradians (circles) and 280 × 10^{-5} steradians (squares) at retinal illuminances of 29.0 T (solid symbols) and 314 T (open symbols).

It is perhaps useful to note three differences in the response patterns for small and large targets under different retinal illuminances. First, higher contrasts are required for small targets to reach threshold than for large targets at a given retinal illuminance. Further, as retinal illuminance increases contrast threshold decreases for all target sizes, but the rate of reduction is faster for small targets than it is for large targets (Figure 3). Second, as target contrast increases just above threshold, reaction times decrease rapidly, but at a slower rate for small targets than for large targets at a given retinal illuminance. As retinal illuminance increases, this initial slope for the reaction times becomes steeper more quickly for small targets than for large targets. In fact, the initial slope changes very little with retinal illuminance for large targets. Third, although reaction times typically saturate with increasing contrast, they will not saturate as quickly for small targets as for large targets at a given adaptation luminance. Throughout the range of retinal illuminances used in this experiment, reaction times to large targets always saturated; only at high adaptation luminances did reaction times to small targets saturate.

3.2 Increment experiment

Figure 4 shows reaction times, again, for subject 6 who was typical of the 'average' subject. The mean reaction times for the largest (13 × 10^{-5} steradians) and smallest (0.20 × 10^{-5} steradians) targets are shown for various contrasts under the highest (51.5 T) and lowest (0.53 T) retinal illuminances. As with the decrement experiment, there is a rapid reduction in reaction times as contrast increases above threshold. Similarly too, increasing target size and retinal illuminance reduces reaction times and the functions become more 'step-like' in appearance. It should be noted, however, that for the smallest targets and the lowest adaptation luminances, the data do not reach an apparent level of saturation. The changes in the patterns of reaction times are more pronounced here than they are in the decrement experiment because, in the increment experiment, small targets were presented at a lower range of retinal illuminances.

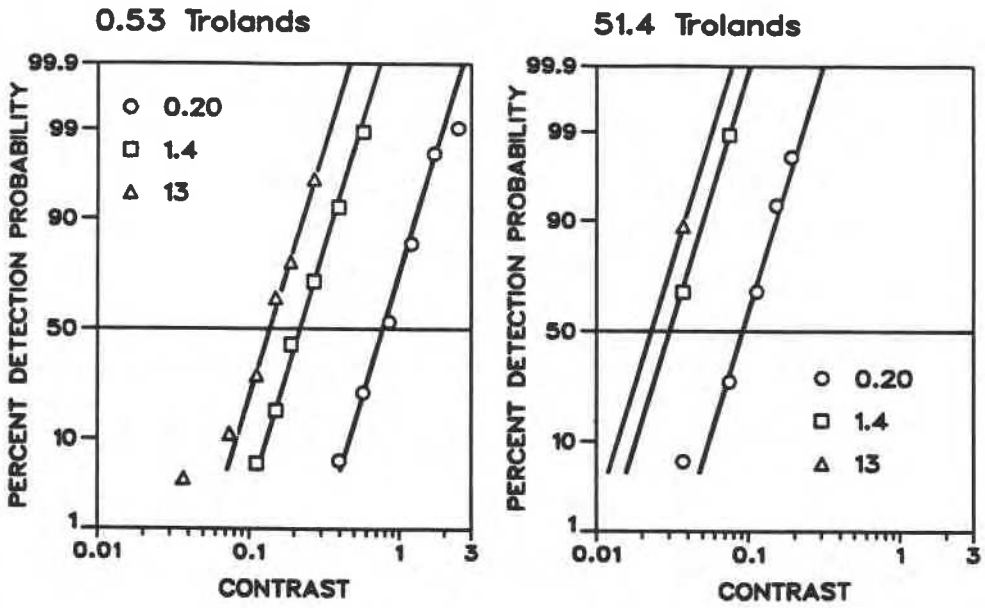

Figure 5 Mean percentage probability-of-detection data for three contrast *increment* target areas (0.20, 1.4, 13×10^{-5} steradians) plotted as a function of $\log_{10}C$ (equation 1) when presented at retinal illuminances of 0.53 and 51.4 T. A straight line (see text) was fitted by eye to *all* of the probability-of-detection data in the increment experiment.

Threshold contrasts for increments were also determined using the probability-of-detection methodology described above for the contrast decrements (Figure 5). Interestingly, the probability of detection versus $\log_{10}C$ data could also be well fitted with straight lines having the same slope as those for the decrement experiment. As with the reaction time data, the changes in the threshold data were more pronounced because of the selected stimulus conditions.

4 Visual performance model

4.1 Contrast threshold

Contrast threshold can be defined as that contrast associated with the 50% probability of detection[19]. Sixty-four average contrast threshold values from the decrement experiment (one for every combination of target area and retinal illuminance) and 15 values from the increment experiment (again, one for every combination of target area and retinal illuminance) were determined (Figures 3 and 5) and combined into one set. Several studies have shown that over the range of adaptation levels used in these two experiments contrast thresholds for increments and decrements on luminous backgrounds are very nearly the same‖[20].

Figure 6 shows the close similarity in the average contrast thresholds for the three target sizes common to both experiments. The solid lines are from equation 2, the form of which is somewhat arbitrary for describing the empirical data. The coefficients in Equation 2 were determined by a least squares, multiple regression routine and best describe the data using this form. This exercise provided a three-dimensional surface, with contrast threshold varying as a function of target area and retinal illuminance. Over 99% of the variance† in the contrast threshold data was accounted for by this equation‡.

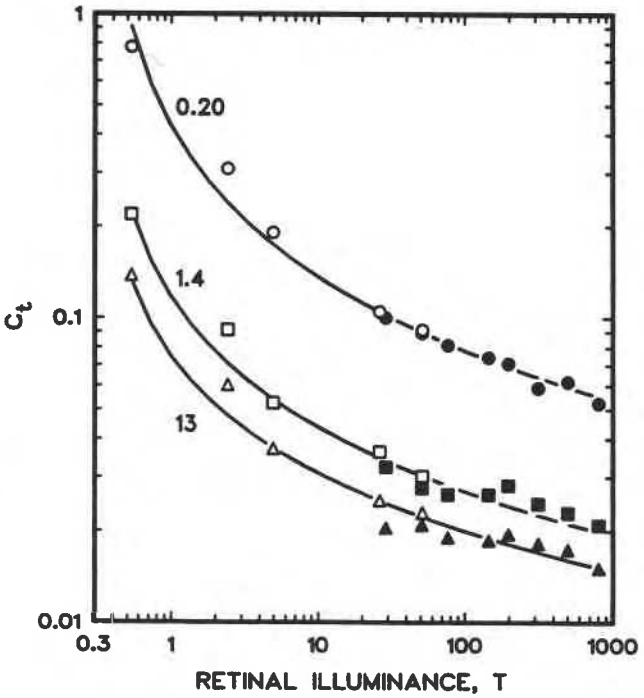

Figure 6 Contrast thresholds C_t plotted as a function of retinal illuminance (T) for the increment (open symbols) and the decrement (closed symbols) experiments. Presented are the averaged data for target areas of 0.20, 1.4 and 13×10^{-5} steradians, which were common to both experiments. The solid lines are the predicted curves for these target areas from equation 2.

‖ Actually, threshold contrast for increments are just slightly higher than they are for decrements but the differences are small, except at very low adaptation (scotopic) levels.

† This is the value, in percent, of the multiple correlation coefficient and is the proportion of the total variance explained by the fitted $\log_{10}$ contrast threshold model in Equation 2.

‡ It should be noted that there is an expected rod-cone break at a retinal illuminance of about 1 troland (21). Indeed there is evidence for this rod-cone separation in this experiment. The three contrast threshold values at an retinal illuminance of 2.42 T in Figures 6 and 7 are consistently above the contrast surface regression lines. This is a result of including the lowest three points at an retinal illuminance of 0.53 T in the contrast surface regression. Thus, some of these points were probably obtained at a high mesopic adaptation level. A more precise model would have to be developed to account for the contrast threshold data obtained near the rod-cone break.

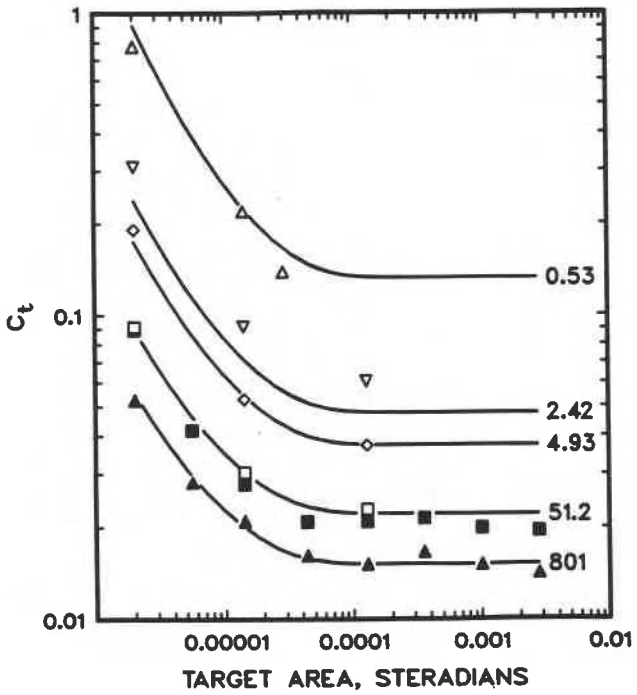

Figure 7 Contrast threshold C_t plotted as a function of target area, in steradians, for the increment (open symbols) and decrement (closed symbols) experiment. Presented are averaged data for five selected retinal illuminances (0.53 to 801 T). The solid lines are the predicted curves for these retinal illuminances from equation 2.

Figures 6 and 7 show two perspectives of this contrast threshold surface together with some of the data.

$$\log_{10}C_t = -1.36 - 0.179A - 0.813L + 0.226A^2 - 0.0772L^2 + 0.169AL \quad (2)$$

where C_t is contrast threshold; $A = \log_{10}(\tanh 20000\omega)$; ω is the area of the target, in steradians, from 0.20 to 280×10^{-5}; $L = \log_{10}(\log_{10}(10\ I_R/\pi))$; I_R is the retinal illuminance, in $(T) = L_a\ \pi\ r^2$; r is the pupil radius (mm) = 1 mm; L_a is the adaptation luminance in cd m^{-2} from 0.17 to 255.

Figure 6 shows a consistent drop in contrast threshold with retinal illuminance for all target areas, although the rate of reduction is greater at the lower retinal illuminances and for the smaller target areas. These trends are consistent with countless studies of contrast threshold (e.g. Reference 19).

Figure 7 shows the relationship between contrast threshold and target area. There is an obvious reduction in contrast threshold up to a target area of about 13×10^{-5} steradians; after that, threshold did not change much, if at all, with target area. Savoy and McCann[22] and Hoekstra *et al*[23] showed that contrast thresholds for low spatial frequencies do not vary as long as the number of cycles presented is the same. In this experiment, flashed squares of different sizes may be considered as half-cycle targets of different spatial frequencies. Thus, the number of cycles for targets of different sizes was always the same. By this interpretation, and in agreement with these earlier studies, these results show that half-cycle targets larger than 0.77 cycles per degree (Table 7) have the same contrast threshold.

4.2 Suprathreshold response

Following the formulation by Rea[6] and Rea *et al*[14] and using the estimates of contrast threshold C_t from Equation 2, Equation 3 can be used to establish a functional relationship between reaction times and target contrasts for a given target area and retinal illuminance. Since visual performance is generally taken as increasing with stimulus strength, it is appropriate to use the reciprocal of reaction times to describe performance. Consequently, Equation 3 employs R, the reciprocal of the average reaction time RT, as the dependent variable.

$$R = [\Delta C^n/(\Delta C^n + K^n)]R_{max} \quad (3)$$

where R is the performance (ms^{-1}) = 1/RT; RT = mean reaction time (ms); $\Delta C = C - C_t$; C is the contrast of the target of a given area and at a given retinal illuminance (equation 1); C_t is the contrast threshold (equation 2) for a given target area and retinal illuminance; K is the value of ΔC corresponding to half-of-maximum response for a given retinal illuminance and target area, that is, a dimensionless free parameter affecting the shape of the response function; n is a dimension free parameter, also affecting the shape of the response function; R_{max} is the maximum possible response for a given retinal illuminance; a free parameter.

Data from both experiments were combined into a set of seventy-nine 'average' reaction times (64 sets for the decrement experiment plus 15 for the increment experiment). Each 'average' reaction time was weighted by the number of trials contributing to that mean. Seventy-nine non-linear regression calculations employing equation 3 produced seventy-nine values of R_{max}, n, and K. Thus, there were estimates of these three parameters for every combination of target area and retinal illuminance used in the two experiments (Appendix A).

Table 4 of Appendix A clearly shows that K varied with target area and retinal illuminance. It was not so clear from Tables 3 and 5 whether n and R_{max} followed any consistent trends with these two independent variables. Figure 14 shows the median estimates of n and R_{max} from the non-linear regressions (equation 3) for each level of retinal illuminance and target area.

Based upon these plots and simple correlation calculations, it was inferred that the parameter n does not vary as a function of retinal illuminance (Figure 14(a)) nor of target area (Figure 14(b)). Thus, a constant value of 0.97 based upon the average value in Table 3 was assumed for n (although a value of 1.0 would probably serve as well and thus simplify equation 3).

There was a significant relationship, however, between R_{max} and retinal illuminance, given the high correlation between them shown in Figure 14(c), but there is no obvious relationship between R_{max} and target area. Thus R_{max} was considered independent of target area, but it was assumed to increase linearly with retinal illuminance according to equation 4:

$$R_{max} = 0.000196 \log_{10}I_R + 0.00270 \quad (4)$$

where I_R is defined in equation 2.

Since the three parameters in equation 3 are not completely independent, changes to the values of n and R_{max} might affect the values of K. Therefore estimates of K were obtained again using the non-linear regression routine, but now assuming that $n = 0.97$ and R_{max} increased with $\log_{10}I_R$ according to equation 4. The seventy-nine new estimates of K are given in Table 6.

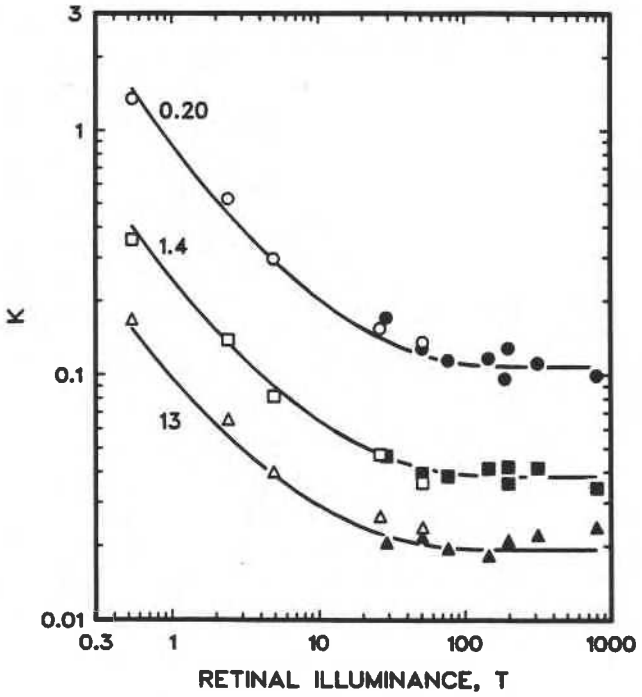

Figure 8 *K* plotted as a function of retinal illuminance (T) for the increment (open symbols) and decrement (closed symbols) experiment. Presented are the averaged data for target areas of 0.20, 1.4 and 13 × 10^{-5} steradians, which were common to both experiments. The solid lines are predicted curves for the target areas from equation 5.

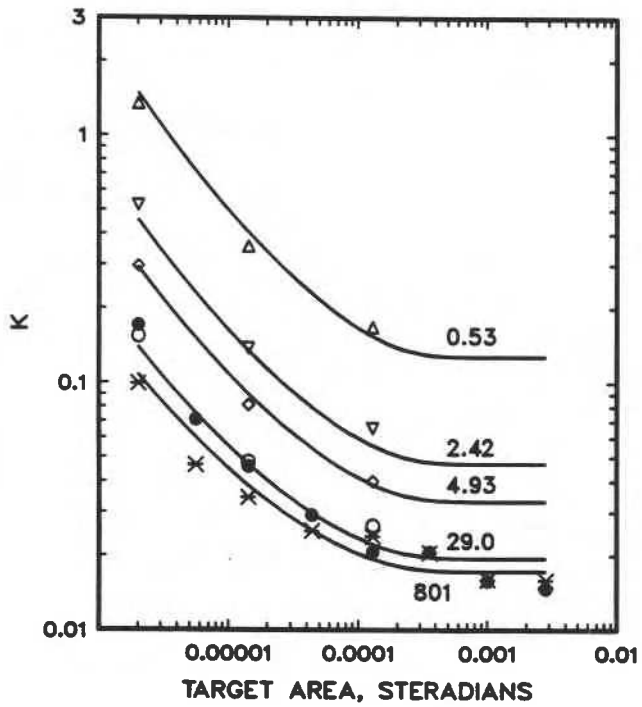

Figure 9 *K* plotted as a function of target area (in steradians) for the increment (open symbols) and decrement (closed symbols and asterisks) experiments. Presented are data for selected retinal illuminances (0.53 to 801 T). The solid lines are the predicted curves for these retinal illuminances from equation 5.

Employing essentially the same procedures used to estimate the contrast threshold surface, it was possible to determine a surface for the new estimates of *K* in Table 6. Equation 5 describes the three-dimensional regression surface for *K* as a function of retinal illuminance and target area; over 99% of the variance in the *K* values was explained by equation 5. It should be noted that this function differs slightly from equation 2 because the *K* values did not continue to decrease with retinal illuminance as had the contrast threshold values. Figures 8 and 9 show different perspectives of the *K* surface.

$$\log_{10}K = -1.76 - 0.175A^* - 0.0310L^* + 0.112A^{*2} + 0.171L^{*2} + 0.0622A^*L^* \quad (5)$$

where *K* is the half saturation parameter (from equation 3 and Table 6 of Appendix A); $A^* = \log_{10}\tanh(5000\omega)$; ω is the target area (steradians) from 0.20 × 10^{-5} to 280 × 10^{-5}; $L^* = \log_{10}\tanh(0.04 I_R/\pi)$; I_R is the retinal illuminance from Equation 2.

Using equations 2 to 5 it is possible to describe all reaction time data from threshold to saturation for the complete range of target contrasts and sizes and retinal illuminances used in the two experiments. Figures 10 and 11 show some data with the comparable predictions generated from the model given by equations 2 to 5. Although all data and the predictions are not shown, Figures 10 and 11 adequately represent the level of predictive accuracy possible. Appendix B compares the predictive accuracy of equations 2 to 5 with that obtained from the seventy-nine independent regressions which lead to the parameter estimates in Tables 3 to 5 (i.e. using just equations 2 and 3). In general, little accuracy is lost by simply using equations 2 to 5, rather than all seventy-nine independent regression equations.

4.3 Visual response

The reaction time data modelled by equations 2 to 5 are not based upon visual response alone. Although probably small, there are both motor and cognitive response times contributing to the reaction times. To model visual performance it is necessary to eliminate these non-visual response times from the data. Rea *et al*[14] assumed that the non-visual contributions to the reaction time data are, on average, constant. If this assumption is true, then the differences in visual response times, ΔT_{vis}, produced by changes in stimulus parameters in this experiment can be determined by subtracting a constant value, equal to the fastest estimated reaction time, RT_{ref}, from each value of RT. By this operation, the non-visual components cancel and the remainder is assumed to be simply the difference in visual response time caused by a change in the stimulus parameters. Therefore, if

$$RT = T_{vis} + T_{non\text{-}vis} \quad (6)$$

where RT is reaction time (ms); T_{vis} is the visual component of RT (ms); $T_{non\text{-}vis}$ is the non-visual component of RT (ms) then

$$\Delta T_{vis} = RT_{ref} - RT \quad (7)$$

where ΔT_{vis} is the incremental visual response time needed to process a stimulus relative to that under reference conditions. RT_{ref} is the reference reaction time which, for this experiment, is the shortest estimated reaction time derived from equation 3 for a retinal illuminance of 801 T and a target size of 280 × 10^{-5} steradians with $n = 0.97$ and R_{max} following

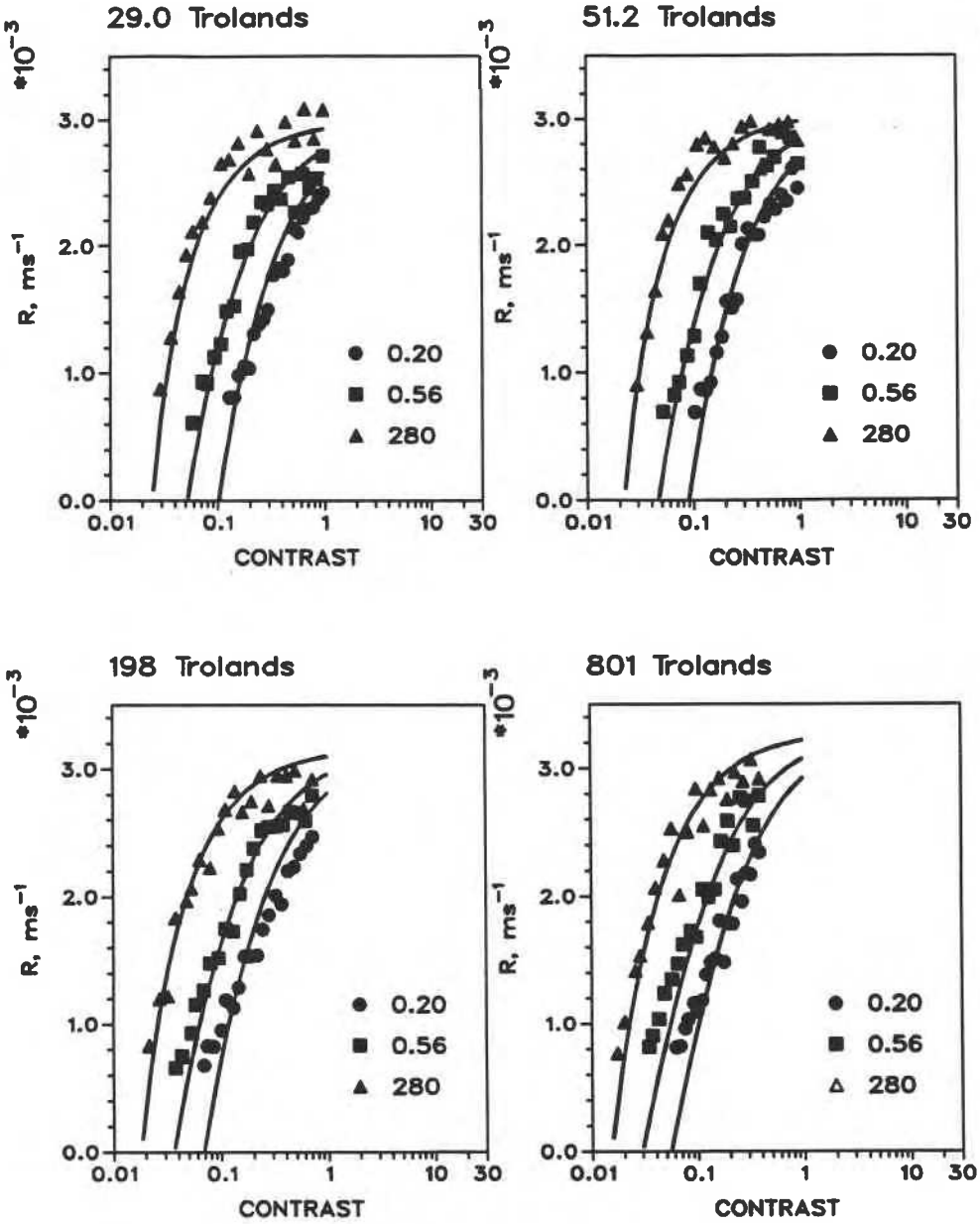

Figure 10 Values of R, the inverse of reaction time, from the *decrement* experiment and averaged over all subjects. The curves were calculated using equations 2 to 5, and are labelled in terms of target area, in steradians $\times 10^5$. Retinal illuminance values are specified above each panel.

equation 4, = 305 ms, thus, following equation 3,

$$\Delta T_{vis} = RT_{ref} - (\Delta C^n + K^n)/(\Delta C^n R_{max}) \quad (8)$$

Figures 12 and 13 show predictions from the visual performance model as defined by equation 8. The model predicts visual performance at a wide range of retinal illuminances, target sizes and contrasts, both luminous decrements and increments. It should be noted that this model predicts differences in visual processing time (ΔT_{vis} in ms), not relative visual performance (RVP) as in Rea[9]. A subsequent publication will discuss the differences in the two measures of visual performance.

5 Discussion

Threshold and suprathreshold visual performance can be described by a few equations. Equation 2 describes the contrast threshold (C_t) surfaces, that is, the break point between seeing and not seeing a target on a luminous background as a function of target area and retinal illuminance. As noted earlier, estimates of this surface have been obtained using a variety of psychophysical techniques (e.g. Reference 24), but there is an artefact in some of the estimates. Only when an equal number of spatial cycles are presented can the relative visual sensitivity to different target areas be correctly determined[22,23]. In the present experiments only spatial half-cycles were presented and, indeed, contrast threshold was the same for square targets larger than 0.65° on a side (13×10^{-5} steradians) or 0.77 cycles per degree, confirming and slightly extending the literature in the area of contrast threshold.

Equation 5 describes the K surface for reaction times as a function of target area and retinal illuminance. Values of K, like C_t, are based upon a constant criterion response. In this case the response criterion is half of the maximum possible reaction time response R_{max} for that adaptation level. To the

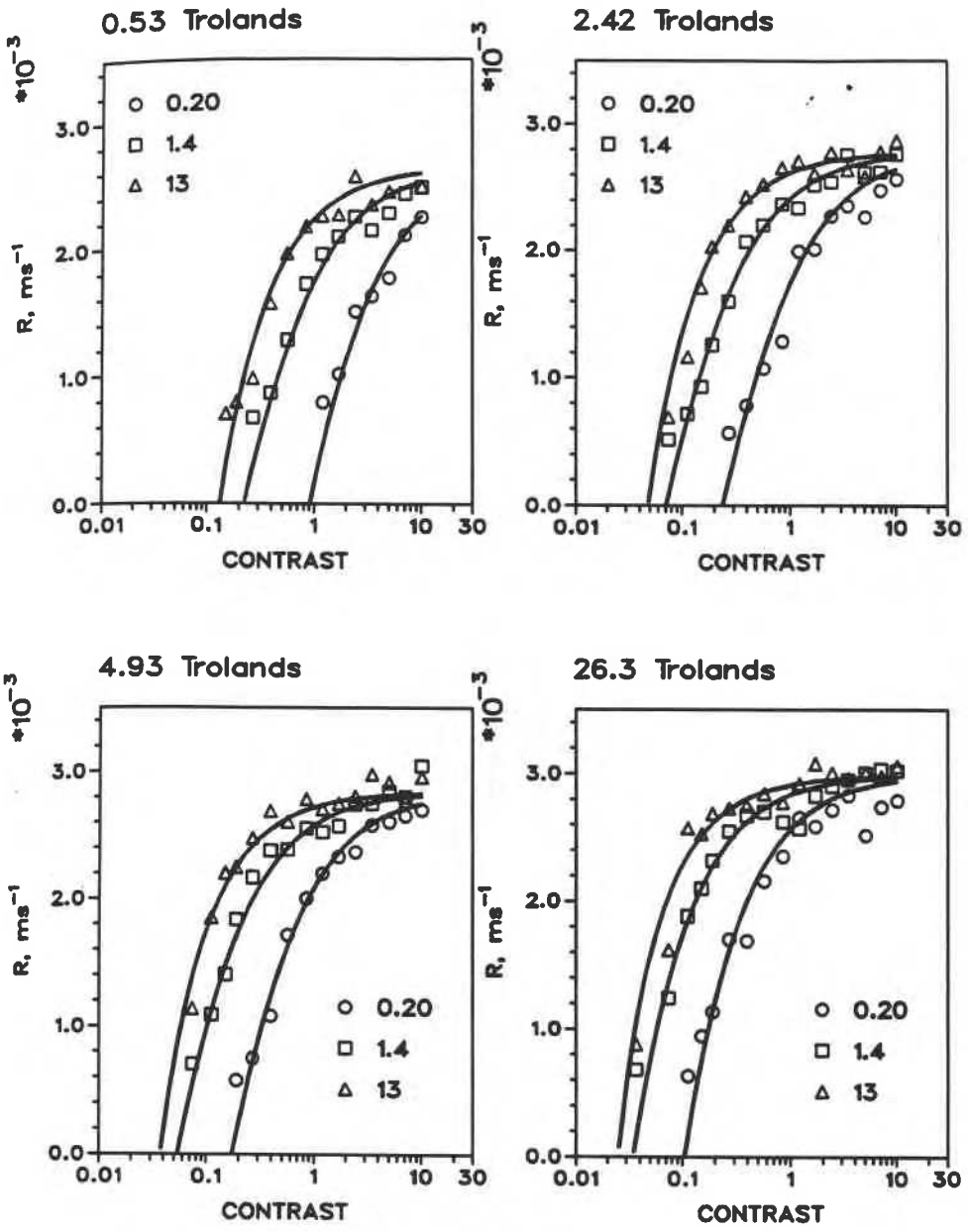

Figure 11 Values of R, the inverse of reaction time, from the *increment* experiment and averaged over all subjects. The curves were calculated using equations 2 to 5, and are labelled in terms of target area, in steradians $\times 10^5$. Retinal illuminance values are specified above each panel.

authors' knowledge, estimates of this surface have never been reported previously.

Figures 12 and 13 show different slices through the visual performance model defined by equation 8. These are views of the 'pure' visual response. The trends are also consistent with other published estimates of visual performance[14] but go beyond them by describing visual performance over a wide range of stimulus conditions.

In general, visual performance improves with target area, target contrast and adaptation luminance. For many combinations of the three model parameters, however, visual performance changes very little and, under these conditions, defines the visual performance plateau and escarpment described by Boyce and Rea[2]. The escarpment is more pronounced and the plateau flatter and larger at the higher adaptation luminances and for the larger target sizes. For many applications the stimulus conditions will be found on this plateau, but, no doubt, under certain circumstances this will not be the case. For example, under some low illumination levels it may be impossible to read small text. It should also be emphasised that the plateau is not perfectly flat, but falls off gradually to the escarpment. Even small reductions in visual performance on the plateau may have large economic significance if they result in productivity decline. For tasks requiring a large amount of visual processing (e.g. inspection of manufactured products) even slightly reduced illumination levels, task contrast or size may be very expensive. In any event, these equations allow, for the first time, precise estimates of visual performance under a wide range of stimulus conditions commonly found in commercial and industrial environments.

6 Conclusions

Three fundamental problems remain in applying these equations, however. First, all data from these two experi-

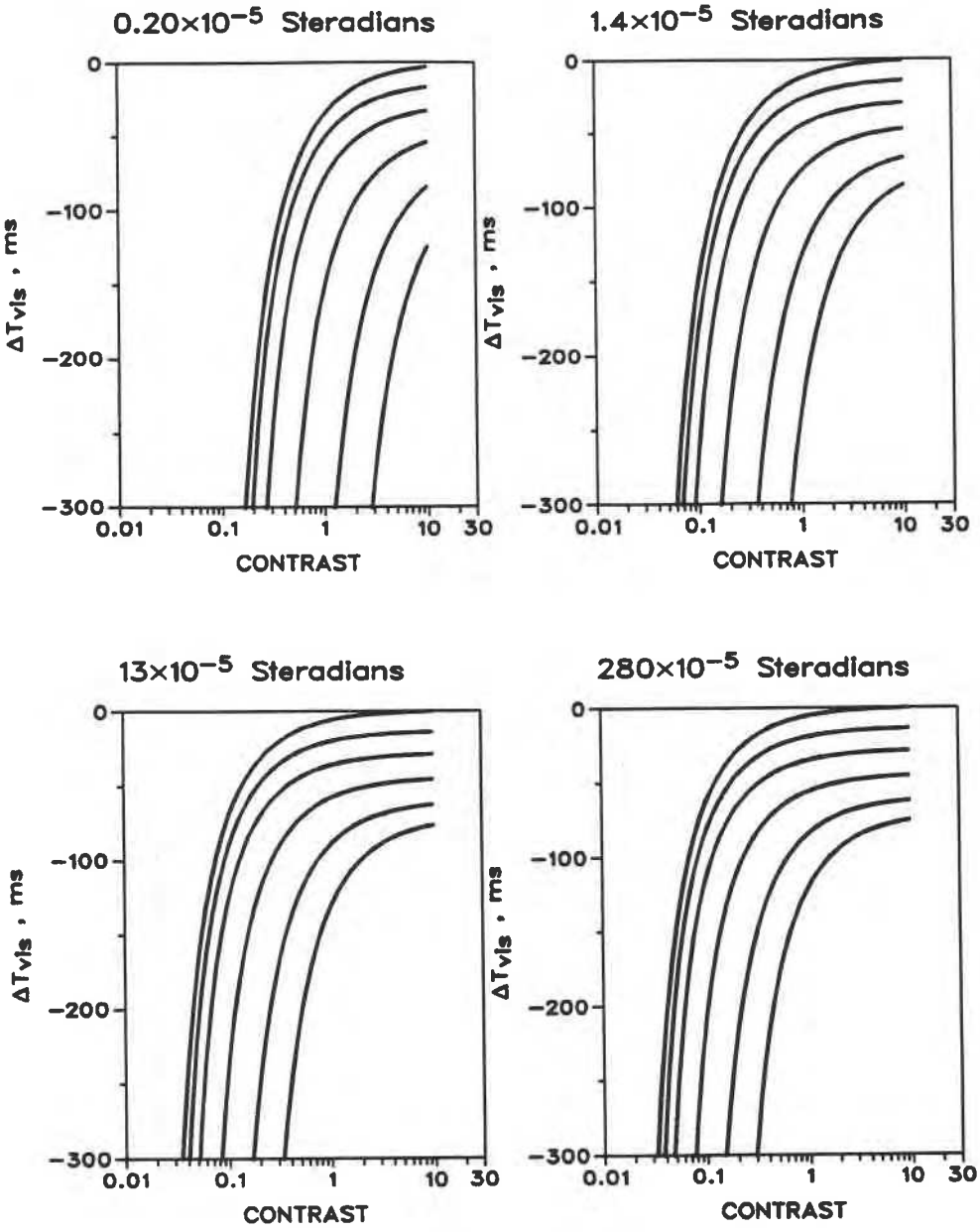

Figure 12 Relative losses in visual performance time ΔT_{vis} (ms) plotted as a function of target contrast for different target areas specified above each panel. The curves are defined by equation 8. They represent, from right to left in every panel, the following retinal illuminances: 0.63, 1.6, 6.3, 31, 160, and 801 T.

ments come from young adults viewing the stimuli through a 2 mm artificial pupil. Since retinal illuminance will depend upon the size of the natural pupil and since pupil size depends upon adaptation luminance as well as the age of the person, it is not possible to predict accurately visual performance using these equations without some estimation of the luminance-dependent and age-dependent pupil size. Further, there is some debate as to whether the deterioration in visual performance with age (e.g. Reference 8) is dependent upon changes to the optical system or to the retina and brain[25]. Unpublished work extending the paper by Wright and Rea indicates that these age-dependent changes in visual performance are due primarily to optical changes, at least up to age 60 or 65 years. Until these arguments and the age-dependent changes in pupil size are published, however, the algorithm in Appendix C has limited utility for predicting visual performance under real conditions.

Second, the practitioner cannot easily measure the input parameters (luminance, target size, and target contrast) for the various equations. Although beyond the scope of this report, a system has been developed at the National Research Council Canada which will provide practical means of measuring these input parameters for actual tasks[16–18]. This system and a set of equations based on this report will allow practitioners to determine visual performance with very little difficulty in the very near future.

Finally, even with a well defined theoretical framework for visual performance and practical means of measuring the stimulus conditions, it will still be necessary to assess the relevance of visual performance to the performance of real tasks. Such understanding goes far beyond the scope of visual sciences and illuminating engineering and into such areas as audition, thermal comfort, ergonomics, motivation,

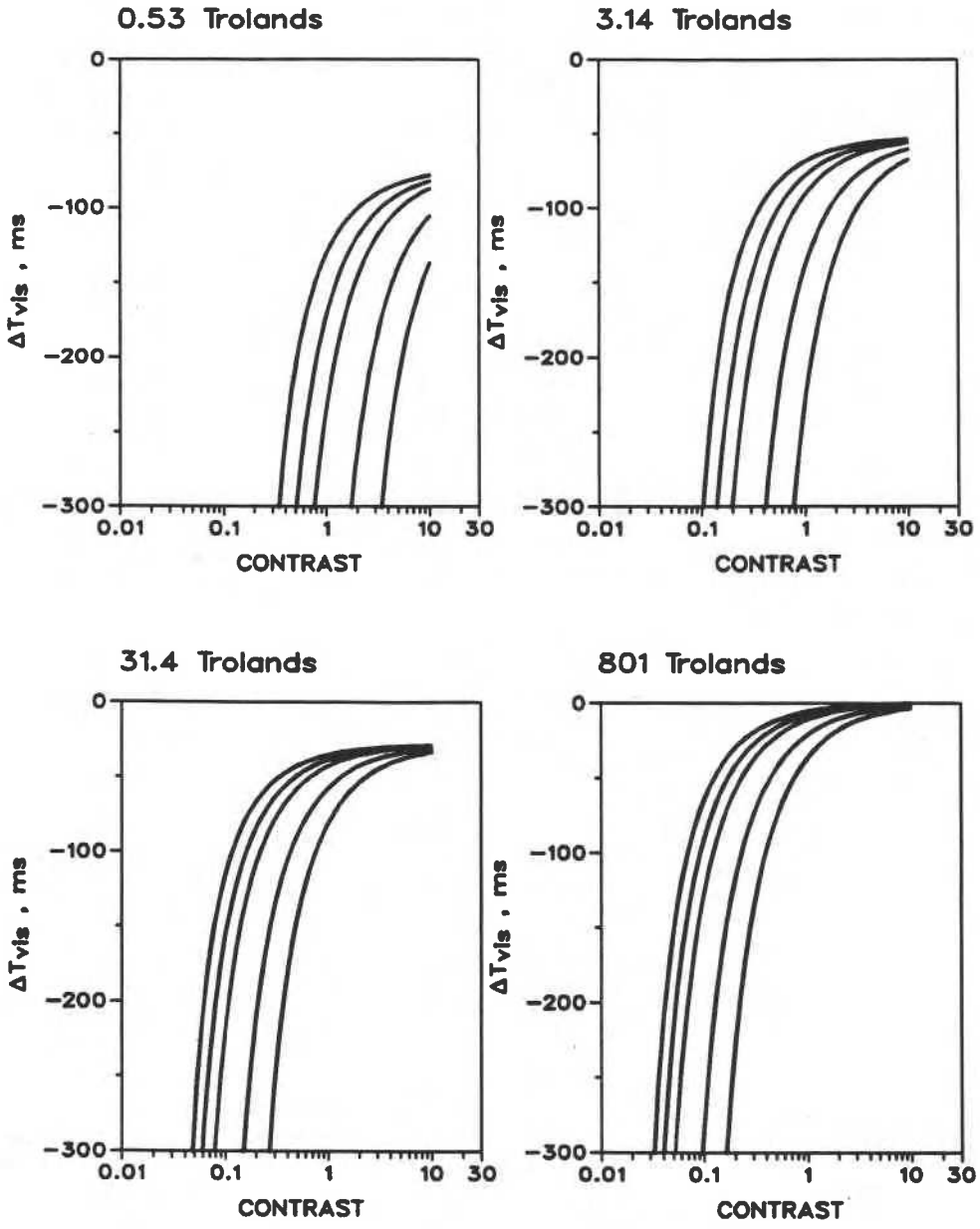

Figure 13 Relative losses in visual performance time ΔT_{vis} (ms) plotted as a function of target contrast for different retinal illuminances specified above each panel. The curves are defined by equation 8. They represent, from right to left in every panel, the following target areas: 0.2, 0.5, 2.0, 5.0 and 280×10^{-5} steradians.

Table 3 Values of the parameter n, collected in both the increment (+) and decrement (−) experiments, obtained from the seventy-nine three-parameter regressions.

I_R(T)	Target area (steradians × 10^5)								
	0.20	0.56	1.4	4.4	13	36	100	280	
0.53	***		0.77		0.79				(+)
2.42	0.73		0.89		1.27				(+)
4.93	0.78		0.92		1.23				(+)
26.3	0.70		0.64		1.11				(+)
29.0	***	0.87	1.07	1.02	1.13	1.17	1.02	0.93	(−)
51.2	0.70	0.86	1.10	1.13	0.93	1.30	1.19	1.35	(−)
51.5	0.88		1.20		1.49				(+)
77.0	0.80	0.88	1.25	1.15	0.87	1.38	0.90	0.77	(−)
145	0.72	0.80	1.32	0.88	1.04	1.12	0.97	1.05	(−)
198	***	0.57	0.63	0.91	0.91	0.99	0.86	0.90	(−)
314	0.99	0.84	1.37	1.04	1.12	1.10	1.33	1.29	(−)
496	0.60	***	0.83	0.72	0.90	1.15	0.93	1.13	(−)
801	***	***	0.73	0.71	0.73	0.87	0.89	0.76	(−)

fatigue, learning, and aesthetics. Thus, while we may have a robust understanding of the impact of lighting and task conditions on visual performance, accurate assessments of productivity, job satisfaction and absenteeism are still not available. Nevertheless, in the very near future practitioners will be able to precisely measure and calculate the impact of lighting and task conditions on visual performance. This capability should place the lighting practitioner at the forefront of application engineering.

Appendix A

The regression parameters n, K and R_{max} were obtained from the non-linear regression (equation 3) routine employing the reaction times (averaged over all subjects). These values are summarised in Tables 3 to 5 and Figure 14. For some combinations of retinal illuminance and target area the non-linear regressions provided very large estimates of R_{max} (i.e. the functions did not saturate). Since the corresponding estimates of n and K are not independent of this parameter,

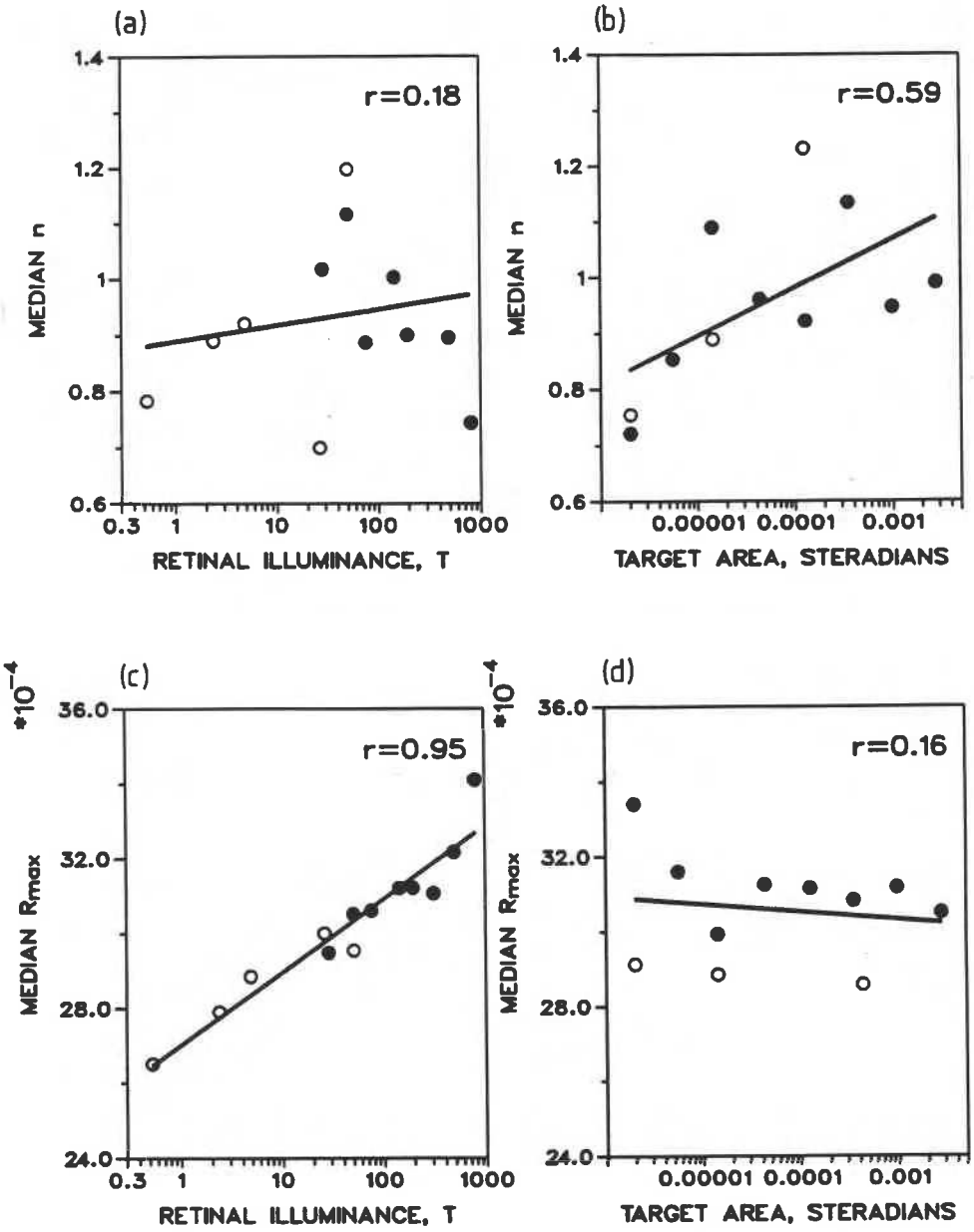

Figure 14 Median values of n and R_{max} are presented as functions of retinal illuminance or target area. Correlation coefficients, r, are shown inset. Equation 4 describing the line in (c) is presented in the text. Open symbols are from the increment experiment. Closed symbols are from the decrement experiment.

Table 4 Values of the parameter K collected in both the increment (+) and decrement (−) experiments, obtained from the seventy-nine, three-parameter regressions.

I_R(T)	Target area (steradians × 10^5)								
	0.20	0.56	1.4	4.4	13	36	100	280	
0.53	***		0.317		0.154				(+)
2.42	0.528		0.136		0.071				(+)
4.93	0.292		0.085		0.049				(+)
26.3	0.126		0.039		0.030				(+)
29.0	***	0.061	0.040	0.028	0.020	0.023	0.018	0.015	(−)
51.2	0.158	0.061	0.040	0.026	0.022	0.022	0.016	0.016	(−)
51.5	0.127		0.042		0.032				(+)
77.0	0.139	0.052	0.038	0.025	0.022	0.021	0.014	0.015	(−)
145	0.128	0.055	0.037	0.029	0.018	0.018	0.016	0.014	(−)
198	***	0.091	0.057	0.026	0.017	0.019	0.016	0.015	(−)
314	0.092	0.050	0.039	0.027	0.023	0.023	0.017	0.016	(−)
496	0.116	***	0.034	0.028	0.021	0.018	0.014	0.016	(−)
801	***	***	0.038	0.030	0.033	0.021	0.016	0.014	(−)

Table 5 Values of the parameter R_{max} collected in both the increment (+) and decrement (−) experiments, obtained from the seventy-nine, three-parameter regressions and reported as $R_{max} \times 10^5$

$I_R(T)$	Target area (steradians $\times 10^5$)								
	0.20	0.56	1.4	4.4	13	36	100	280	
0.53	***		264		266				(+)
2.42	288		279		274				(+)
4.93	291		289		286				(+)
26.3	297		311		300				(+)
29.0	***	290	283	295	289	299	306	303	(−)
51.2	334	313	299	291	306	305	309	292	(−)
51.5	291		296		298				(+)
77.0	335	303	295	296	324	303	309	317	(−)
145	332	323	289	318	307	307	320	305	(−)
198	***	376	357	308	302	312	317	305	(−)
314	300	319	300	317	317	314	307	301	(−)
496	352	***	326	335	322	310	315	309	(−)
801	***	***	347	358	372	335	335	327	(−)

they were excluded from Tables 3 to 5 (***). Functions for all seventy-nine data sets were obtained, however, and estimates of the mean square errors are presented in Appendix B.

Appendix B

Table 8 presents the mean-square errors (MSEs) obtained from the seventy-nine regressions which lead to the estimates of n, K and R_{max} in Tables 3 to 5 of Appendix A. Also presented are the MSEs for the same data sets obtained from the predictions generated by equations 2 to 5. The seventy-nine independent regressions are expected to be more accurate predictions of the data. Indeed, this is true (except for some cases where the iteration criterion was reached with slightly less variance explained), but the improvements are small in most cases.

The model predictions are poorest and the MSEs most disparate for the smallest sizes or where a veiling luminance was

Table 7 Sizes, in various units, of the square targets used in the decrement and increment experiments

Degrees	Steradians $\times 10^5$	Cycles per degree
0.08	0.20	6.1
0.14	0.56	3.6
0.22	1.4	2.3
0.38	4.4	1.3
0.65	13	0.77
1.1	36	0.46
1.8	100	0.27
3.0	280	0.16

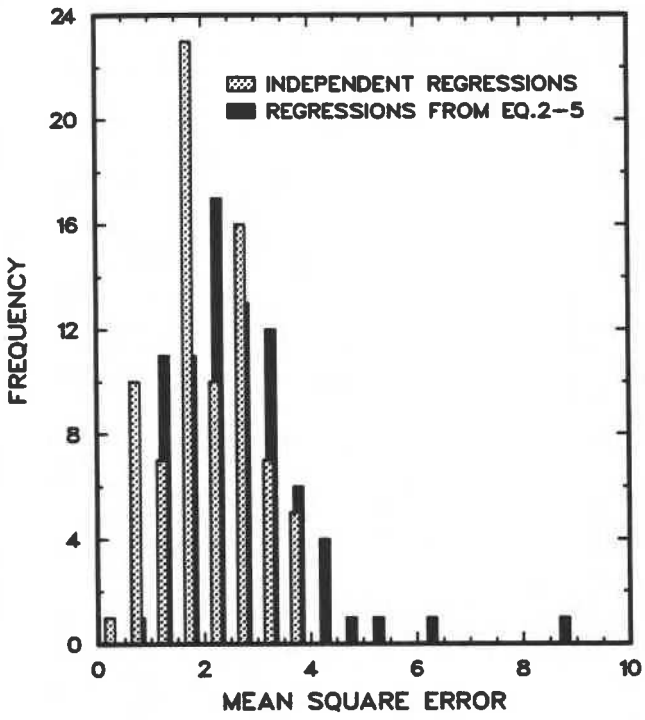

Figure 15 Distributions of mean square error (multiplied by a factor of 10^8) obtained from the independent, non-linear regressions and from the regressions using equations 2 to 5.

Table 6 Values of the parameter K collected in both the increment (+) and decrement (−) experiments. These values were obtained from a one-parameter non-linear regression (equation 3) with n constant at 0.97 and R_{max} varying according to equation 4.

$I_R(T)$	Target area (steradians $\times 10^5$)								
	0.20	0.56	1.4	4.4	13	36	100	280	
0.53	1.345		0.355		0.168				(+)
2.42	0.521		0.138		0.065				(+)
4.93	0.295		0.081		0.040				(+)
26.3	0.153		0.047		0.026				(+)
29.0	0.170	0.071	0.046	0.029	0.020	0.020	0.015	0.014	(−)
51.2	0.127	0.058	0.039	0.028	0.021	0.019	0.013	0.014	(−)
51.5	0.135		0.036		0.023				(+)
77.0	0.114	0.058	0.038	0.026	0.019	0.017	0.014	0.016	(−)
145	0.116	0.053	0.041	0.028	0.018	0.018	0.014	0.015	(−)
198	0.128	0.056	0.042	0.029	0.021	0.019	0.016	0.017	(−)
314	0.111	0.054	0.041	0.027	0.022	0.023	0.016	0.017	(−)
496	0.096	0.049	0.036	0.028	0.022	0.019	0.016	0.017	(−)
901	0.099	0.046	0.034	0.025	0.023	0.020	0.016	0.015	(−)

Table 8 Mean-square errors (MSEs) multiplied by a factor of 10^8. The top entry for each combination of retinal illuminance I_R and target area is the MSE obtained from the independent, non-linear regression exercise; the bottom entry is the mean-square error obtained from the prediction generated by equations 2 to 5. The MSE values are presented as a frequency histogram in Figure 15.

I_R(T)	Target area (steradians × 10^5)							
	0.20	0.56	1.4	4.4	13	36	100	280
0.53	0.85		1.3		2.6			
	2.6		2.1		2.7			
2.42	2.9		2.1		0.76			
	3.2		1.9		1.3			
4.93	2.0		1.3		0.72			
	2.1		1.1		1.2			
26.3	2.6		2.2		1.7			
	4.5		2.9		1.8			
29.0	0.55	1.9	1.0	2.3	1.8	1.8	2.0	1.4
	1.6	2.5	1.2	2.1	1.8	2.2	2.1	1.3
51.2	1.6	2.6	0.73	2.0	2.3	2.8	1.7	1.4
	2.6	2.4	0.80	2.0	2.0	3.9	2.6	2.0
51.5	2.9		0.82		0.61			
	3.1		1.2		1.3			
77.0	1.9	3.0	1.0	3.5	2.8	3.9	2.5	2.8
	1.9	3.1	1.4	3.3	2.8	4.5	2.3	2.8
145	0.49	1.9	1.7	2.0	3.3	3.6	1.9	2.5
	1.5	2.1	2.1	1.8	3.0	3.3	1.9	2.3
198	1.6	2.0	1.6	3.7	2.6	3.1	3.6	1.9
	8.8	4.1	3.2	3.7	3.4	2.8	3.4	2.5
314	0.88	2.4	1.6	1.8	2.6	1.6	2.9	3.2
	1.1	2.7	2.4	1.7	2.5	1.5	3.4	3.8
496	1.3	2.8	2.2	2.8	3.5	2.9	2.1	3.1
	4.8	3.6	2.5	4.0	3.3	2.9	2.3	3.1
801	1.3	1.5	1.7	1.8	2.9	3.6	3.1	2.5
	6.4	5.1	2.7	2.4	3.2	3.3	2.9	3.8

employed. Under these conditions it was difficult to see response saturation clearly in the data and, very likely, the larger disparities are caused by relatively poor estimates of the saturation parameter R_{max}. Since the relatively large MSEs are few (Figure 15), the estimations from equations 2 to 5 (Figures 10 and 11) are probably adequate for describing the reaction times.

Appendix C

Algorthim for calculating predicted performance R and incremental visual performance time ΔT_{vis} from measurements of retinal illuminance (I_R in trolands from 0.53 to 801), stimulus area (ω, in steradians from 2×10^{-6} to 2.8×10^{-3}), and contrast (C).

Step 1: Calculate contrast threshold C_t

$A = \log_{10} \tanh (20000\omega)$

$L = \log_{10} \log_{10} (10\, I_R/\pi)$

I_R = Retinal illuminance from 0.53 to 801 T
$= L_a\, \pi\, r^2$

r = Pupil radius (mm)

L_a = Adaptation luminance (cd m^{-2})

ω = Area of target (steradians) from 2.0×10^{-6} to 2.8×10^{-3}

$$\log_{10} C_t = -1.36 - 0.179A - 0.813L + 0.226A^2 - 0.772L^2 + 0.169AL$$
$$-0.0772$$

Step 2: Calculate the half-saturation constant K

$A^* = \log_{10} \tanh (5000\omega)$

$L^* = \log_{10} \tanh (0.04 I_R/\pi)$

$$\log_{10} K = -1.76 - 0.175A^* - 0.0310L^* + 0.112A^{*2} + 0.171L^{*2} + 0.0622A^*L^*$$

Step 3: Calculate maximum response R_{max}

$$R_{max} = 0.00196 \log_{10} I_R + 0.00270$$
$$0.000196$$

Step 4: Calculate performance R *and predicted reaction time* RT

$\Delta C = C - C_t$

$$R = \frac{\Delta C^{0.97}}{\Delta C^{0.97} + K^{0.97}} R_{max}$$

$RT = 1/R$

Step 5: Calculate predicted reaction time RT_{ref} *for a reference stimulus condition*

For $A > 13 \times 10^{-5}$ steradians, $I_R = 801$ T, and $C > 1$, $RT_{ref} = 305$ ms.

Step 6: Calculate the change in visual performance ΔT_{vis} *relative to the reference condition described in Step 5.*

$\Delta T_{vis} = RT_{ref} - RT$

Acknowledgements

The authors would like to thank the nine subjects who participated in the experiment and Mr I Jeffry who designed the computer software for running the experiments. This study was financially supported, in part, by Public Works Canada. The authors are particularly grateful to Mr Ivan Pasini who was the Project Manager for the financial assistance from Public Works Canada and instrumental in realising the project to completion.

References

1 Levy A W The role of visual performance in lighting design and specification *Public Works Canada Conf. Proc. The integration of visual performance criteria into the illumination design process, Ottawa, Canada* (1982)
2 Rea M S *J. Illum. Eng. Soc.* **16** 128 (1987)
3 Rea M S *Lighting Res. Technol.* **18** 113 (1986)
4 Weston H C *The relation between illumination and industrial efficiency, 1. The effect of size of work* (London: Industrial Health Research Board of the Medical Res. Council and Illumination Res. Committee of the Dept. Scientific and Industrial Research/His Majesty's Stationery Office) (1935)
5 Weston H C *The relation between illumination and visual efficiency — the effect of brightness contrast* (London: Industrial Health Research Board of the Medical Res. Council) (1945)
6 Rea M S *J. Illum. Eng. Soc.* **15** 41 (1986)

7 Smith S W and Rea M S Relationships between office task performance and ratings of feelings and task evaluations under different light sources and levels *Proc. 19th Session of the CIE, Kyoto, Japan* (1980)
8 Rea M S *J. Illum. Eng. Soc.* **10** 164 (1981)
9 Slater A I, Perry M J and Crisp V H C The applicability of the CIE visual performance model to lighting design *Proc. 20th Session of the CIE, Amsterdam, Netherlands* (1983)
10 Perry M J, Slater A I and Gong-Xia Y Illuminance and uniformity — Their effects on the performance of a realistic visual task *Proc. Nat. Lighting Conf. Nottingham, England* (1986)
11 Luce R D *Response times* (Oxford: Clarendon) (1986)
12 Welford A T *Reaction times* (London: Academic) (1980)
13 Boyce P R and Rea M S Plateau and escarpment: The shape of visual performance *Proc. 21st Annual Session CIE, Venice, Italy* (1987)
14 Rea M S, Boyce P R and Ouellette M J *Lighting Res. Technol.* **19** 101 (1987)
15 McNelis J F *J. Illum. Eng. Soc.* **2** 190 (1973)
16 Rea M S and Jeffrey I G *CapCalc: A new luminance and image analysis system for lighting and vision* National Research Council Canada, Institute for Research in Construction, Publication IR 565 (1988)
17 Kambich D G and Rea M S *Lighting Magazine* **1**(3) 16 (1987)
18 Rea M S *Architectural Lighting* **1**(11) 30 (1987)
19 Blackwell H R *J. Opt. Soc. Amer.* **36** 624 (1946)
20 Short A D *J. Physiol.* **185** 646 (1966)
21 Hecht S, Peskin J C and Patt M *J. Gen. Physiol* **22** 7 (1938)
22 Savoy R L and McCann J J *J. Opt. Soc. Amer.* **65** 343 (1975)
23 Hoekstra J, van der Groot D P J, van den Brink G and Bilsen F A *Vision Res.* **14** 365 (1974)
24 Kelly D H *Optica Acta* **24** 107 (1977)
25 Wright G A and Rea M S *Proc. International Conf. Occupational Ergonomics Volume 1: Research reports and case studies* Human Factors Conference, Inc., Rexdale, Ontario, 508 (1984)